Analysis of an Overmoded Re-entrant cavity

David Marques-Villarroya, Felipe Penaranda-Foix, Beatriz Garcia-Banos, Jose Manuel Catala-Civera,
Jose Daniel Gutierrez-Cano
ITACA Research Institute
Universitat Politècnica de València
Valencia, Spain
damarvi3@itaca.upv.es, fpenaran@dcom.upv.es, beagarba@itaca.upv.es, jmcatala@dcom.upv.es, jdgutierrez@itaca.upv.es

***Abstract*—A rigorous analysis of an over-moded re-entrant cavity is performed in this paper in order to provide a complete modal solution, taking into account the whole set of modes, TE, TM and TEM, instead of the classical models which only consider TM_{0np}. The used method is a combination of mode-matching technique and circuit analysis, obtaining the flexibility of the circuit technique and the accuracy of the mode-matching method. The behavior of some resonant modes, in relation with the air gap of the inner conductor, has been studied for the full-wave case. Some experimental measurements of azimuthal variation modes with empty cavity have been also performed to validate the accuracy of the proposed analysis. Furthermore, dielectrometry simulations have been carried out, comparing the results with other methods of the literature and with commercial numerical techniques (FEM).**

Keywords—Mode-matching, circuit analysis, re-entrant cavity, full wave, dielectrometry.

I. INTRODUCTION

The re-entrant cavity is one of the most used cavities in the microwave technology because of its wide tuning range and high sensibility. It has been used to develop dielectrometers [1], transducers [2], tunable combline resonators [3] - [4], medical applicators [5], etc.

For resonant applications, the gap of the inner conductor produces the concentration of electric field in that region, and its behavior is similar to a capacitor [6]. For this reason, the most common resonant modes used in this type of cavities are TM_{0np}, and most models are developed taking into account only those set of modes [7] – [9].

However, other modes can be used, especially in applications where a broadband measurement is important. For example, in [10] is shown how to use the hybrid HE_{11} mode in the re-entrant cavity for a Gunn oscillator application and the study of semiconductors. This paper goes further, since we analyze the re-entrant cavity with full-wave method, taking into account all the set of modes (TEM, TE_{mnp} and TM_{mnp}). The main goal of this paper is the modeling of the re-entrant cavity with all kind of resonant modes in order to extend the range of applicability of the current models, which mostly make use of only the TM_{0np}.

There are many configurations of the re-entrant cavity, but we are going to focus only in the single re-entrant cavity (Fig. 1).

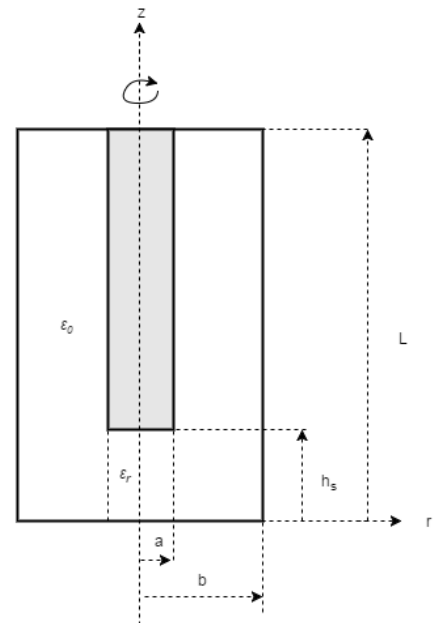

Fig.1. Single re-entrant cavity geometry.

The theoretical model is explained in section II. In section III some results are presented such as mode charts, measurements, simulations and comparisons with other publications and methods.

II. THEORY

The modeling of this cavity has been performed combining *mode-matching* technique and circuit analysis. Both methods have already been used separately to model this type of cavity successfully in [7] and [9], but taking into account only the TM_{0np} modes. Our purpose consists of taking the best of each method to model the re-entrant cavity with *full-wave* technique in the easiest way, getting a good accuracy with the optimal computational time. We have called this procedure *mode-matching circuital full-wave (MMCFW).*

In order to analyze the structure, it is divided into two regions: Region 1, $(0 < r < a) \cap (0 < z < h_s)$; Region 2, $(a < r < b) \cap (0 < z < L)$.

It is well known how to write the electric and magnetic fields in both regions [11]. It is important to emphasize that we take into account all the set of modes (TEM, TE_{mnp} and

TM$_{mnp}$). We have included TEM modes as a particular case of TM mode. To be more specific, the TM$_{00p}$ modes represent the TEM resonant modes, when they exist.

On the interface r=a, the transverse electric and magnetic fields are approximated by a series expansion of basis functions (such as generalized circuit technique):

$$E_z^{(1)}\Big|_{r=a} = \sum \alpha_z \cdot e_z \qquad E_z^{(2)}\Big|_{r=a} = \sum \alpha_z \cdot e_z$$
$$E_\varphi^{(1)}\Big|_{r=a} = \sum \alpha_\varphi \cdot e_\varphi \qquad E_\varphi^{(2)}\Big|_{r=a} = \sum \alpha_\varphi \cdot e_\varphi \tag{1}$$

$$H_z^{(1)}\Big|_{r=a} = \sum \beta_z \cdot h_z \qquad H_z^{(2)}\Big|_{r=a} = \sum \beta_z \cdot h_z$$
$$H_\varphi^{(1)}\Big|_{r=a} = \sum \beta_\varphi \cdot h_\varphi \qquad H_\varphi^{(2)}\Big|_{r=a} = \sum \beta_\varphi \cdot h_\varphi \tag{2}$$

where E and H are the electric and magnetic field inside of each region; while e and h are the basis functions employed in the interface; and α and β are the weights of the basis functions.

Applying the orthogonality properties of the basis functions, we achieve the expression of the weights, in function of the amplitudes of each region.

$$\alpha_z = A_{ez} a_1^{TM} \qquad \alpha_z = B_{ez} a_2^{TM}$$
$$\alpha_\varphi = A_{e\varphi}^{TM} a_1^{TM} + A_{e\varphi}^{TE} a_1^{TE} \qquad \alpha_\varphi = B_{e\varphi}^{TM} a_2^{TM} + B_{e\varphi}^{TE} a_2^{TE} \tag{3}$$

$$\beta_z = A_{hz}^{TE} a_1^{TE} \qquad \beta_z = B_{hz}^{TE} a_2^{TE}$$
$$\beta_\varphi = A_{h\varphi}^{TM} a_1^{TM} + A_{h\varphi}^{TE} a_1^{TE} \qquad \beta_\varphi = B_{h\varphi}^{TM} a_2^{TM} + B_{h\varphi}^{TE} a_2^{TE} \tag{4}$$

Where, a_1 and a_2, are the unknown amplitudes of electromagnetic fields in regions 1 and 2 respectively. For each region, both TM and TE modes are considered, then, the problem is modeled with the amplitudes a_1^{TM}, a_1^{TE}, a_2^{TM} and a_2^{TE}. And, A and B are the modal matrices.

Now, we equal the weights of the basis functions in both sides of the interface to enforce the boundary conditions, achieving a system equation, which corresponds with the well-known eigenvalue problem that appears in the pure *mode-matching* method. The dimension of the problem is related directly to the number of modes employed in each region.

$$\underbrace{\begin{pmatrix} A_{hz} & 0 & -B_{ez} & 0 \\ A_{e\varphi}^{TM} & A_{e\varphi}^{TE} & -B_{e\varphi}^{TM} & -B_{e\varphi}^{TE} \\ 0 & A_{hz}^{TE} & 0 & -B_{hz}^{TE} \\ A_{h\varphi}^{TM} & A_{h\varphi}^{TE} & -B_{h\varphi}^{TM} & -B_{h\varphi}^{TE} \end{pmatrix}}_{X} \begin{pmatrix} a_1^{TM} \\ a_1^{TE} \\ a_2^{TM} \\ a_2^{TE} \end{pmatrix} = 0 \tag{5}$$

In order to solve the eigenvalue problem, we need to set the determinant of the matrix X to zero and solve the resonant equation:

$$|\det(X)| = 0 \tag{6}$$

III. Results

In re-entrant cavities is especially interesting to study the resonant frequency shift with the empty cavity (ε_r=1), in relation with the height of the gap (h_s), because of its easy tunability [12]. We have performed some simulations to study this effect with different modes.

The height gap range has been chosen to cover the entire height of the cavity (h_s=*[0, L]*). Thus, in the first and last point, we have analytical solutions of the resonant frequency, because the structure becomes a circular coaxial cavity with h_s=0, and a regular circular cavity with h_s =*L*, which resonant frequencies have analytical expressions [11].

In the proper re-entrant cavity, with a gap, the modes can be symmetric (TM$_{0np}$-TE$_{0np}$) or hybrids, where both E_z and H_z appear, though one of them is always more significant than the other. Then, we can distinguish *Quasi~TM* modes, whose H_z component is very small, but not negligible, and E_z has greater contribution; and *Quasi~TE* modes, whose E_z component is very small, but not negligible, and H_z has a greater contribution.

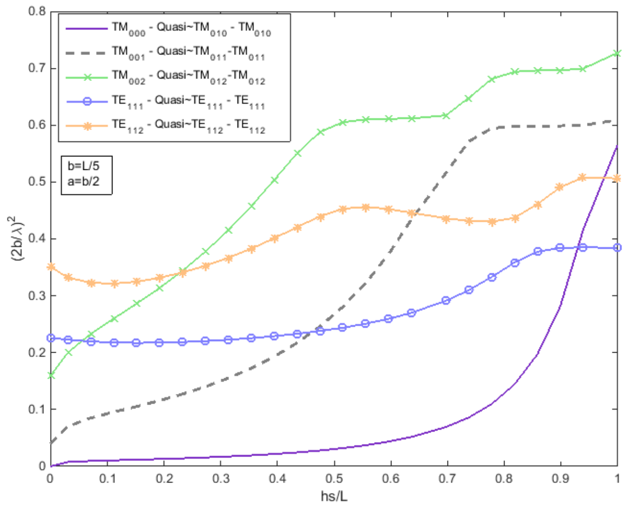

Fig. 2. Mode chart of the re-entrant cavity with the height gap (h_s) as variable. *b=L/5 & a=b/2*

Following the resonant frequencies with the height gap variation (h_s), we have achieved some interesting mode charts (Fig. 2 and 3), where one can see the behavior of some resonant modes in the re-entrant cavity. The simulations have been performed for two different of geometries, with different aspect ratio (L/b). In Fig. 2, L/b =5, therefore, TE resonant modes appear first than TM and TEM; in Fig. 3, L/b =1/5, therefore, TEM and TM resonant modes appear first than TE.

Only the first resonant modes are shown to facilitate the readability. We have identified each mode with the following notation (legend of mode charts):

"Mode with h_s=0 – Mode with 0< h_s <L – Mode with h_s =L". When the X appears, it means that the resonant mode does not exist in the coaxial case (h_s=0).

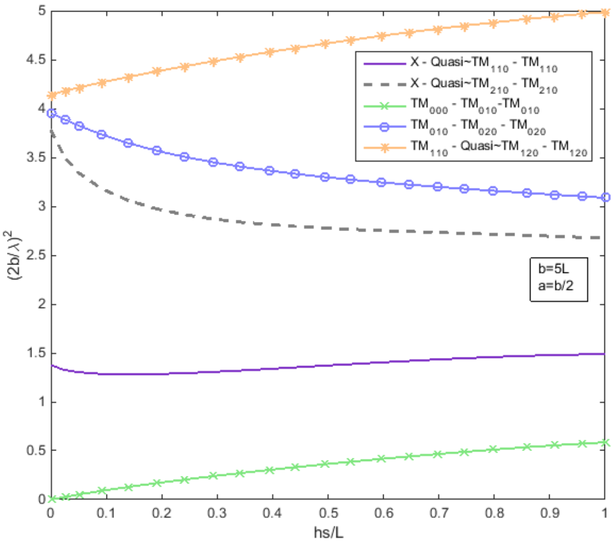

Fig.3. Mode chart of the re-entrant cavity with the height gap (h_s) as a variable. *b=5L & a=b/2*

In Fig. 2 and 3, we can see how the resonant TEM modes (TM_{00p}) of the coaxial cavity (h_s=0), become TM_{0np} in the re-entrant cavity with a gap and remains as TM_{0np} in the circular cavity ($h_s=L$). The TE modes of the coaxial cavity (h_s=0), become *Quasi*~TE modes when the gap increases, and get back to the pure TE mode in the circular case ($h_s=L$). The TM modes have a particular behavior in this type of cavities. On the one hand, the *Quasi~*TM_{m1p} modes of the re-entrant cavity, do not have an equivalent coaxial mode, they appear only when there is a gap, and become pure TM_{m1p} on $h_s=L$ (circular case). On the other hand, the TM_{mnp} modes of the coaxial cavity, become *Quasi*~$TM_{m(n+1)p}$ when the gap appears, and remain as $TM_{m(n+1)p}$ when $h_s=L$ (circular case). This effect occurs because TEM modes of the coaxial cavity, become TM_{0np} when the gap appears, thus, a displacement in the radial coordinate (index *n* of the TM_{mnp} modes) takes place.

In order to validate the model, we have performed some experimental measurements of the resonant frequency with empty cavity. The comparison between the proposed method and the measurement is shown in Table I, where one can see that the relative differences are less than 0.5% in all the cases.

TABLE I RESONANT FREQUENCIES OF EMPTY CAVITY.
b=40 mm; a=17.5 mm; L=118 mm; h_s=78 mm.

Mode	fr – Meas.	fr – MMCFW	Δfr (%)
TM_{011}	2.962107	2.966936	0.16
Quasi~TM_{111}	2.349514	2.341654	0.33
Quasi~TM_{112}	4.87666	4.882989	0.13

Finally, we are going to show the applicability of this *full-wave* method for dielectrometry. The high sensitivity of the fundamental modes produces a good accuracy in the computation of the material permittivity. Consequently, most of the methods of the literature develop a modeling of the cavity with only TM_{0np} modes. However, the frequency range of permittivity estimation is often too small, because just the first few modes can be measured properly. In order to extend the bandwidth, we propose this model to employ other modes besides the usual TM_{0np}.

Table II shows a comparison between our *full-wave* method (MMCFW), pure *mode-matching* taking into account only TM_{0np} modes [1], and finite differences time domain (FDTD) method commercial software (QuickWave®). We have compared the resonant frequencies of three different materials provide in [1] (for only TM_{010}), with our method and QuickWave®. Furthermore, we have added two more resonant frequencies for each material, which are not TM_{0np}, they are azimuthal variation modes. In those cases, the comparison is only between QuickWave® and MMCFW.

TABLE II RESONANT FREQUENCIES WITH DIELECTRIC LOADED GAP.
b=2.56 cm; a=0.75 cm; L=2 cm; h_s=0.5 cm.

ε_r	Mode	fr [1]	fr (MMCFW)	fr (QuickWave®)	Δfr (%)
2,495	TM_{010}	1,9741	1,975	1,9702	0,0455
	Quasi~TM_{110}	NA	6,2434	6,2426	0,0123
	Quasi~TE_{211}	NA	9,1239	9,1254	0,0164
3,734	TM_{010}	1,7284	1,7285	1,7284	0,0057
	Quasi~TM_{110}	NA	5,7513	5,7514	0,0017
	Quasi~TM_{121}	NA	8,3117	8,3116	0,0012
30,83	TM_{010}	0,6969	0,6965	0,6966	0,0573
	Quasi~TM_{110}	NA	2,4757	2,4804	0,1894
	Quasi~TM_{210}	NA	4,1372	4,1482	0,2651

The relative differences in the computation of the resonant frequencies, calculated with three different methods, is less than 1% in all the cases, providing a good agreement between them.

IV. CONCLUSION

A *full-wave* study of the re-entrant cavity has been performed with a new mixture technique combining *mode-matching* and circuit methods, providing a really good accuracy in the resolution of resonant problems.

Two mode charts with different aspect ratio have been presented in order to predict the behavior of some resonant modes (TEM, TE_{mnp} and TM_{mnp}) with an empty cavity, in relation with the height gap.

Some experimental measurements of symmetrical modes and azimuthal variation modes have been performed to validate our method with the empty cavity.

A dielectrometry application has also been shown, where the estimation of the resonant frequency of re-entrant cavity with dielectric-loaded gap has been compared with other techniques of the literature, using the fundamental mode (TM_{010}), and with commercial numerical software (EMPro) to obtain the resonant frequencies of higher-order modes. The results show a good agreement with other techniques, validating the model presented in this paper.

Acknowledgment

This work has been financially supported by "Programa de Ayudas de Investigación y Desarrollo (PAID) de la Universitat Politècnica de València", "Programa de Apoyo a la investigación y Desarrollo (PAID-00-15) de la Universitat Politècnica de València", and by "Conselleria de Educación, Investigación, Cultura y Deporte. Generalitat Valenciana (BEST/2016/012)".

Results are obtained under the project SEDMICRON - TEC2015-70272-R (MINECO/FEDER), financed by Ministerio de Economía y Competitividad (MINECO) - Spanish Government- and by European Regional Development Funds (ERDF) of European Union.

References

[1] W. Xi, W. R. Tinga, W. A. G. Voss and B. Q. Tian, "New results for coaxial re-entrant cavity with partially dielectric filled gap," in IEEE Transactions on Microwave Theory and Techniques, vol. 40, no. 4, pp. 747-753, Apr 1992.

[2] Y. Fan, Z. Zhang, N. C. Carvalho, J. M. Le Floch, Q. Shan and M. E. Tobar, "Investigation of Higher Order Reentrant Modes of a Cylindrical Reentrant-Ring Cavity Resonator," in IEEE Transactions on Microwave Theory and Techniques, vol. 62, no. 8, pp. 1657-1662, Aug. 2014.

[3] Chi Wang, Hui-Wen Yao and K. A. Zaki, "Modeling of re-entrant coaxial and combline resonators and filters," IEEE Antennas and Propagation Society International Symposium. 1996 Digest, Baltimore, MD, USA, 1996, pp. 280-283 vol.1.

[4] R. Lech, A. Kusiek and J. Mazur, "Analysis of circular cavity with tunable combline resonator," 15th Conference on Microwave Techniques COMITE 2010, Brno, 2010, pp. 175-178.

[5] T. Yabuhara et al., "Finite Element Analysis of the Re-entrant Type Resonant Cavity Applicator for Brain Tumor Hyperthermia," 2007 29th Annual International Conference of the IEEE Engineering in Medicine and Biology Society, Lyon, 2007, pp. 3540-3543.

[6] James Baker-Jarvis and Bill F. Riddle, "Dielectric Measurements Using a Reentrant Cavity: Mode-Matching Analysis, " NIST Technical Note 1384, Nov. 1996.

[7] W. Xi and W. R. Tinga, "Field analysis of new coaxial dielectrometer," in IEEE Transactions on Microwave Theory and Techniques, vol. 40, no. 10, pp. 1927-1934, Oct 1992.

[8] R. G. Carter, J. Feng and U. Becker, "Calculation of the Properties of Reentrant Cylindrical Cavity Resonators," in IEEE Transactions on Microwave Theory and Techniques, vol. 55, no. 12, pp. 2531-2538, Dec. 2007.

[9] F. L. Penaranda-Foix, J. M. Catala-Civera, A. J. Canos-Marin and B. Garcia-Banos, "Circuital analysis of a coaxial re-entrant cavity for performing dielectric measurement," Microwave Symposium Digest, 2009. MTT '09. IEEE MTT-S International, Boston, MA, 2009, pp. 1309-1312.

[10] S. Sen, P. K. Saha and B. R. Nag, "Resonant modes in re-entrant cavities," in Radio and Electronic Engineer, vol. 50, no. 3, pp. 113-116, March 1980..

[11] C. A. Balanis, *Advanced Engineering Electromagnetics*. John Wiley & Sons, 1989.

[12] Weiguo Xi, Baiqiang Tian and W. R. Tinga, "Numerical analysis of a movable dielectric gap in coaxial resonators for dielectric measurements," in IEEE Transactions on Instrumentation and Measurement, vol. 43, no. 3, pp. 486-487, Jun 1994.